Synthesis, Bifunctionalization, and Application of Isocyanurate-Based Periodic Mesoporous Organosilicas

Wen-Hua Zhang,[†] Xiaoning Zhang,[†] Zile Hua,[‡] Parala Harish,[†] Felicitas Schroeder,[†] Stephan Hermes,[†] Thomas Cadenbach,[†] Jianlin Shi,[‡] and Roland A. Fischer*[,†]

Organometallics & Materials Chemistry, Inorganic Chemistry II, Ruhr-University Bochum, Bochum D-44780, Germany, and State Key Laboratory of High Performace Ceramics, Shanghai Institute of Ceramics, Chinese Academy of Sciences, Shanghai 20005, China

Received August 15, 2006. Revised Manuscript Received March 13, 2007

Isocyanurate-containing silsesquioxane-bridged periodic mesoporous organosilicas (ICS−PMOs) were synthesized by self-assembly of the nonionic surfactant P123, $EO_{20}PO_{70}EO_{20}$, and trimethoxysilyl-functionalized isocyanurate (ICS−Si) under acidic conditions in the presence of inorganic additives. The ICS−PMOs have been modified by an alkyl-bridged organosilane (i.e., Et−Si; Et = $-CH_2CH_2-$) by substituting ICS−Si with Et−Si in the precursors, at various molar ratios, resulting in bifunctionalized PMOs exhibiting two types of bridged groups (ICS−Et−PMOs). The obtained bifunctionalized ICS−Et−PMOs have been characterized by X-ray diffraction, transmission electron microscopy, nitrogen physical sorption, and solid-state ^{29}Si and ^{13}C magic angle spinning NMR spectroscopy. Experiments show that the ICS−Et−PMOs exhibit hexagonal mesoscopic structures. Increasing the content of the Et−Si functionality in the precursors is found to significantly improve the mesostructural ordering of the product. It is suggested that fluoride anions as additives play an important role in the formation of well-ordered ICS−PMOs and as well the bifunctionalized ICS−Et−PMOs in the presented experiments. The ICS−PMO materials were used to chemically adsorb H_2PtCl_6, and Pt nanoparticles were subsequently prepared within the mesopores of ICS−PMO by $NaBH_4$ reduction in solution, highlighting the simplicity in exploiting the application of such PMOs in nanomaterials fabrication.

Introduction

First introduced in 1999,[1] periodic mesoporous organosilicas (PMOs) have gained increasing interest because of their highly tunable properties by varying the R group in the bridged organosilane precursors $(R'O)_3-Si-R-Si-(OR')_3$.[2] To date, PMOs with simple bridging groups derived from methane,[3] ethane,[4] ethylene,[5] acetylene,[6] phenyl and its derivatives,[7−9] and thiophene[10] have been developed. PMOs were also prepared from a three-membered cyclic organosiloxane, $[(EtO)_2Si(CH_2)]_3$,[11] and alkoxysilyl-functionalized dendrimers.[12] Recently, Jaroniec et al. have incorporated trimethoxysilyl-functionalized isocyanurate (ICS−Si) into mesoporous silicas using ICS−Si and tetraethyl orthosilicate (TEOS) as coprecursors.[13] The highest content of the ICS groups incorporated is less than 25 mol %, and the frameworks of such hybrid materials mainly consisted of SiO_2. Prominently, Jaroniec's ICS-containing mesoporous materials show a strong ability to adsorb Hg^{2+}, making ICS-based PMOs very attractive. More recently, these researchers have incorporated ICS−Si into the frame-

* To whom correspondence should be addressed. Phone: +49-(0)234 32-24174. Fax: +49-(0)234 32-14174. E-mail: roland.fischer@ruhr-uni-bochum.de.
[†] Ruhr-University Bochum.
[‡] Chinese Academy of Sciences.

(1) (a) Inagaki, S.; Guan, S.; Fukushima, Y.; Ohsuna, T.; Terasaki, O. *J. Am. Chem. Soc.* **1999**, *121*, 9611. (b) Asefa, T.; MacLachan, M. J.; Coombs, N.; Ozin, G. A. *Nature* **1999**, *402*, 867. (c) Melde, B. J.; Holland, B. T.; Blanford, C. F.; Stein, A. *Chem. Mater.* **1999**, *11*, 3302.

(2) (a) Kickelbick, G. *Angew. Chem., Int. Ed.* **2004**, *43*, 3102. (b) Hunks, W. J.; Ozin, G. A. *J. Mater. Chem.* **2005**, *15*, 3716. (c) Hoffmann, F.; Cornelius, M.; Morell, J.; Froeba, M. *Angew. Chem., Int. Ed.* **2006**, *45*, 3216. (d) Hatton, B.; Landskron, K.; Whitnall, W.; Perovic, D.; Ozin, G. A. *Acc. Chem. Res.* **2005**, *38*, 305.

(3) (a) Asefa, T.; MacLachlan, M. J.; Grondey, H.; Coombs, N.; Ozin, G. A. *Angew. Chem., Int. Ed.* **2000**, *39*, 1808. (b) Zhang, W.-H.; Daly, B.; O'Callaghan, J.; Zhang, L.; Shi, J-L.; Li, C.; Morris, M. A.; Holmes, J. D. *Chem. Mater.* **2005**, *17*, 6407. (c) Bao, X.-Y.; Li, X.; Zhao, X.-S. *J. Phys. Chem. B* **2006**, *110*, 2656.

(4) (a) Liang, Y.; Hanzlik, M.; Anwander, R. *Chem. Commun.* **2005**, 525. (b) Guo, W.; Park, J.-Y.; Oh, M.-O.; Jeong, H.-W.; Cho, W.-J.; Kim, I.; Ha, C.-S. *Chem. Mater.* **2003**, *15*, 2295. (c) Bao, X. Y.; Zhao X. S.; Li, X.; Chia, P. A.; Li, J. *J. Phys. Chem. B* **2004**, *108*, 4684. (d) Liang, Y.; Hanzlik, M.; Anwander, R. *J. Mater. Chem.* **2006**, *16*, 138.

(5) (a) Nakajima, K.; Lu, D. L.; Kondo, J. N.; Tomita, I.; Inagaki, S.; Hara, M.; Hayashi, S.; Domen, K. *Chem. Lett.* **2003**, *32*, 950. (b) Asefa, T.; Kruk, M.; MacLachlan, M. J.; Coombs, N.; Grondey, H.; Jaroniec, M.; Ozin, G. A. *J. Am. Chem. Soc.* **2001**, *123*, 8520. (c) Xia, Y.; Wang, W.; Mokaya, R. *J. Am. Chem. Soc.* **2005**, *127*, 790. (d) Xia, Y.; Yang, Z.; Mokaya, R. *Chem. Mater.* **2006**, *18*, 1141.

(6) Yoshina-Ishii, C.; Asefa, T.; Coombs, N.; MacLachlan, M. J.; Ozin, G. A. *Chem. Commun.* **1999**, 2539.

(7) (a) Inagaki, S.; Guan, S.; Ohsuna, T.; Terasaki, O. *Nature* **2002**, *416*, 304. (b) Goto, Y.; Inagaki, S. *Chem. Commun.* **2002**, 2410. (c) Yang, Q.; Kapoor, M. P.; Inagaki, S. *J. Am. Chem. Soc.* **2002**, *124*, 9694.

(8) Kapoor, M. P.; Yang, Q.; Inagaki, S. *J. Am. Chem. Soc.* **2002**, *124*, 15176.

(9) (a) Kapoor, M. P.; Yang, Q.; Inagaki, S. *Chem. Mater.* **2004**, *16*, 1209. (b) Kuroki, M.; Asefa, T.; Whitnal, W.; Kruk, M.; Yoshina-Ishii, C.; Jaroniec, M.; Ozin, G. A. *J. Am. Chem. Soc.* **2002**, *124*, 13886. (c) Cornelius, M.; Hoffmann, F.; Froeba, M. *Chem. Mater.* **2005**, *17*, 6674. (d) Sayari, A.; Wang, W. *J. Am. Chem. Soc.* **2005**, *127*, 12194.

(10) Morell, J.; Wolter, G.; Fröba, M. *Chem. Mater.* **2005**, *17*, 804.

(11) Landskron, K.; Hatton, B. D.; Perovic, D. D.; Ozin, G. A. *Science* **2003**, *302*, 266.

(12) Landskron, K.; Ozin G. A. *Science* **2004**, *306*, 1529.

(13) (a) Olkhovyk, O.; Jaroniec, M. *J. Am. Chem. Soc.* **2005**, *127*, 60. (b) Olkhovyk, O.; Pikus, S.; Jaroniec, M. *J. Mater. Chem.* **2005**, *15*, 1517. (c) Grudzien, , R. M.; Pikus, S.; Jaroniec, M. *J. Phys. Chem. B* **2006**, *110*, 2972.

10.1021/cm061922p CCC: $37.00
Published on Web 04/24/2007

works of so-called ethane-bridged PMOs by diluting ICS−Si in 1,2-bis(triethoxysilyl)ethane (BTSE), resulting in bifunctionalized PMOs consisting of two types of bridged silsesquioxane groups.[14] The content of ICS−Si was reported to be less than 25 mol % to obtain well-ordered mesostrutured materials. Ozin et al. efficiently used the postsynthesis approach to prepare PMOs containing different bridged silsesquioxanes.[15] However, the procedure used in this method is complex; hence, it is not trivial to reproduce the products.

Although significant advances in the synthesis of PMOs have been made, not all bridged silsesquioxane precursors, especially those exhibiting large volumes, are able to self-assemble into well-ordered mesostructures by the surfactant−silicate assembly fashion. It is thus necessary to dilute them with another silica source, e.g., TEOS, to manufacture well-ordered mesostructures.[13,14,16] Moreover, very few studies have been reported on the synthesis of bifunctionalized PMOs using different bridged silsesquioxanes as coprecursors.[14,17] Although successful in specific cases, it is difficult to extend them into a generally efficient synthetic strategy to synthesize bifunctionalized PMOs. It is expected that an efficient approach to prepare well-ordered PMOs using different bridged silsesquioxanes as coprecursors could greatly broaden the scopes, tailor the properties, and exploit the potential applications of multifunctionalized PMOs. The direct synthesis has been demonstrated to be an efficient approach to introduce functional groups into the relatively inert frameworks of PMOs, resulting in materials with one bridging group within the frameworks and one functional group protruding into the mesopores.[5b,7c,18] Although it is possible to efficiently functionalize the surfaces of PMOs by a grafting reaction via a supercritical fluid technique,[3b] the postsynthesis functionalization is not suitable to modify the PMOs with specific functional groups conveniently, limiting their use as catalysts and templates for nanomaterials fabrication.

Despite the remarkable progress in the nanochemistry of mesoporous silicas,[19] very few successes have been made by using PMOs as nanotemplates.[20] This is very likely due to the fact that the pore surfaces of PMOs are comparably inert, making their surface functionalization difficult. The lower thermal stability of PMOs, compared to mesoporous silicas, is another important factor to limit their application. Nevertheless, it has very recently been shown that PMOs are superior to mesoporous silicas as nanotemplates in the formation of highly crystalline Ge nanocrystals.[3b] Therefore, it is desirable to further exploit the nanochemistry of PMOs.

The present study has a 3-fold objective: (i) synthesis of ICS-bridged PMOs (ICS−PMO) using pure ICS−Si as the organosilica precursor, which is a very large functional group with the ability to adsorb metal ions; (ii) exploration of an efficient approach to prepare bifunctionalized PMOs with two types of bridged silsesquioxanes; (iii) exploitation of application for the ICS−PMO in nanomaterials fabrication.[3b,20] Our experiments discussed below show that well-ordered ICS-based PMO materials have been prepared using pure ICS−Si as the organosilica source, $EO_{20}PO_{70}EO_{20}$ (P123) as the template, and NH_4F and NaCl as additives. We have also demonstrated that the bifunctionalized PMOs, consisting of ICS−Si and Et−Si with various component ratios (ICS−Et−PMO), can be synthesized with well-ordered hexagonal pore structures. It is suggested that NH_4F plays the key factor to form well-ordered ICS−Et−PMOs: NH_4F significantly accelerates the hydrolysis rate of Et−Si, to match the rate of ICS−Si.[21] Experiments also revealed that ICS−PMOs can chemically adsorb H_2PtCl_6, without further surface functionalization. Pt nanoparticles were subsequently formed within the mesopores of ICS−PMO by solution reduction.

Experimental Section

(1) Chemicals. Tris[3-(trimethoxysilyl)propyl]isocyanurate (ICS−Si) (Gelest) and 1,2-bis(trimethoxysilyl)ethane (Et−Si) (Aldrich) were used as the bridged organosilica sources. Pluronic P123 ($EO_{20}PO_{70}EO_{20}$) (Aldrich), HCl (aqueous, 37%), and NH_4F and NaCl were used as the structure-directing agent, acid source, and inorganic additives, respectively. $H_2PtCl_6{\cdot}2H_2O$ (Acros) was used to prepare Pt nanocrystals. All chemicals were used as received.

(2) Synthesis. *(a) Synthesis of ICS−PMO in the Presence/Absence of NH_4F in 0.1 M HCl Solution.* The synthetic procedure is mainly based on the previous report on the synthesis of the methane-bridged PMOs.[3b] Typically, 1.25 g of P123 and 3.5 g of NaCl were dissolved in 40 mL of 0.1 M HCl solution in the absence/presence of NH_4F at room temperature. The molar ratio of NH_4F to ICS−Si was kept at 10% (namely, molar ratio $F^-/Si = 3.3\%$) if NH_4F was used. The solution was stirred at 37 °C for at least 5 h before the addition of 2.2 mL of ICS−Si, followed by vigorous stirring for 20 h. The resultant gels were then aged statically at 60 °C for 48 h. The powders were filtered, washed with distilled water, and dried at 60 °C for 20 h. Removal of the surfactants was accomplished by extraction using acidified ethanol.[3b] The final products prepared in the presence/absence of NH_4F in the synthetic media were named ICS−PMO(F) and ICS−PMO(no F), respectively.

(14) Grudzien, R. M.; Grabicka, B. E.; Pikus, S.; Jaroniec, M. *Chem. Mater.* **2006**, *18*, 1722.
(15) Whitnall, W.; Asefa, T.; Ozin, G. A. *Adv. Funct. Mater.* **2005**, *15*, 1696.
(16) (a) Corriu, R. J. P.; Mehdi, A.; Reyé, C.; Thieuleux, C. *Chem. Commun.* **2002**, 1382. (b) Baleizão, C.; Gigante, B.; Das, D.; Alvaro, M.; Garcia H.; Corma, A. *Chem. Commun.* **2003**, 1860. (c) Baleizão, C.; Gigante, B.; Das, D.; Álvaro, M.; Garcia, H.; Corma. A. *J. Catal.* **2004**, *223*, 106.
(17) Morell, J.; Güngerich, M.; Wolter, G.; Jiao, J.; Hunger, M.; Klar, P. J.; Fröba, M. *J. Mater. Chem.* **2006**, *16*, 2809. (c) Jayasundera, S.; Burleigh, M. C.; Zeinali, M.; Spector, M. S.; Miller, J. B.; Yan, W.; Dai, S.; Markowitz, M. A. *J. Phys. Chem. B* **2005**, *109*, 9198. (d) Burleigh, M. C.; Jayasundera, S.; Spector, M. S.; Thomas, C. W.; Markowitz, M. A.; Gaber. B. P. *Chem. Mater.* **2004**, *16*, 3.
(18) (a) Zhu, H.; Jones, D. J.; Zajac, J.; Dutartre, R.; Rhomari, M.; Rozière, J. *Chem. Mater.* **2002**, *14*, 4886. (b) Burleigh, M. C.; Dai, S.; Hagaman, E. W.; Lin, J. S. *Chem. Mater.* **2001**, *13*, 2537. (c) Burleigh, M. C.; Markowitz, M. A.; Spector, M. S.; Gaber, B. P. *J. Phys. Chem.* **2001**, *105*, 9935. (d) Jiang, D.; Yang, Q.; Yang, J.; Zhang, L.; Zhu, G.; Su W.; Li, C. *Chem. Mater.* **2005**, *17*, 6154.
(19) (a) Shi, J. L.; Hua, Z. L.; Zhang, L. X. *J. Mater. Chem.* **2004**, *14*, 795. (b) Zhang, W.-H.; Shi, J.-L.; Wang, L.-Z.; Yan, D.-S. *Chem. Mater.* **2000**, *12*, 1408. (c) Zhang, W.-H.; Shi, J.-L.; Chen, H.-R.; Hua, Z.-L.; Yan, D.-S. *Chem. Mater.* **2001**, *13*, 648. (d) Bronstein, L. M. *Top. Curr. Chem.* **2003**, *226*, 55.
(20) (a) Fukuoka, A.; Sakamoto, Y.; Guan, S.; Inagaki, S.; Sugimoto, N.; Fukushima, Y.; Hirahara, K.; Iijima, S.; Ichikawa, M. *J. Am. Chem. Soc.* **2001**, *123*, 3373. (b) Sakamoto, Y.; Fukuoka, A.; Higuchi, T.; Shimomura, N.; Inagaki, S.; Ichikawa, M. *J. Phys. Chem. B* **2004**, *108*, 853.
(21) Zhang, W.-H.; Lu, J.; Han, B.; Li, M.; Xiu, J.; Ying, P.; Li, C. *Chem. Mater.* **2002**, *14*, 3413.

(b) Synthesis of ICS−PMO under Various Acid Concentrations. This procedure is similar to that for ICS−PMO(F) except that the concentration of HCl solution used was 0.50, 0.25, 0.10, and 0.05 M in each preparation, respectively. The products are correspondingly designated as ICS−PMO(x M) (x = 0.50, 0.25, 0.10, and 0.05). It should be noted that ICS−PMO(0.10 M) is the same as ICS−PMO(F).

(c) Synthesis of Bifunctionalized PMOs Consisting of ICS−Si and Et−Si. For the synthesis of PMOs bridged by ICS−Si and Et−Si, a 0.25 M HCl solution was used, and the overall amount of Si was unchanged for all samples. The molar composition of ICS−Si and Et−Si in the synthesis gel was $(1.0 - x)$ICS−Si:[$(3/2)x$]-Et−Si (x = 0.0, 0.25, 0.50, 0.75, and 1.0), and the products were correspondingly named ICS−Et−PMO($1 - x$). [Note: the sample ICS−Et−PMO(1.0) is the same as ICS−PMO(0.25 M), and Et−PMO is the ICS−Et−PMO(0.0).] All other synthetic conditions and template removal methods are identical to those of ICS−PMO-(F).

(d) Synthesis of Pt Nanocrystals within ICS−PMO(0.10 M). A 0.1 g sample of $H_2PtCl_6 \cdot 2H_2O$ was dissolved in 50 mL of absolute ethanol, and then 0.5 g of ICS−PMO(0.1 M) was added to this solution. After the solution was stirred for 30 min and filtered and the filtrate washed with ethanol, the color of the sample changed from white to yellow, indicating that H_2PtCl_6 had been adsorbed by the ICS−PMO(0.10 M). To remove the H_2PtCl_6 that was physically adsorbed by the ICS−PMO, the yellow powder was added to 100 mL of ethanol, the resulting solution was stirred for 30 min, and then the powder was separated from the solution by filtration and washed with ethanol. The resultant H_2PtCl_6-containing ICS−PMO(0.10 M) was reduced using $NaBH_4$ (0.1 M, 100 mL of ethanol solution) for 30 min. The color of the powder changed from yellow to pale gray. After the powder was separated, washed with ethanol, and dried at room temperature, Pt-containing ICS−PMO (Pt−ICS−PMO) was obtained.

(3) Characterization. X-ray diffraction (XRD) analysis was carried out on a Bruker-D8 Advance X-ray diffractometer, using Cu Kα radiation, operated at 40 kV and 30 mA using capillary mode. Transmission electron microscopy (TEM) was carried out on a JEOL 2010 microscope operating at 200 kV. N_2 sorption isotherms were obtained on a Micrometrics Tristar analyzer. The samples were degassed at 150 °C under nitrogen flow for 6 h before measurement. The pore size distributions (PSDs) were calculated using the Barret−Joyner−Halenda (BJH) method based on the adsorption branches of the sorption isotherms, and the pore sizes were estimated from the positions of the maxima in the PSDs. Solid-state ^{29}Si magic angle spinning (MAS) NMR and ^{13}C MAS NMR were conducted on a Bruker OSX400 WB NMR spectrometer. The ^{29}Si MAS NMR spectra were recorded in a 4 mm ZrO_2 rotor at 79.4 MHz, with a pulse time of 5000 μs, an MAS rate of 10 kHz, and an acquisition time of 17 ms. The ^{13}C CP MAS NMR spectra were measured at 100.6 MHz, with a pulse time of 3000 μs, an MAS rate of 10 kHz, and an acquisition time of 35 ms.

Results and Discussion

(1) Synthesis of ICS−PMO. Figure 1 shows the XRD patterns of the ICS−PMO samples prepared in 0.10 M HCl solution in the presence/absence of NH_4F. The X-ray diffraction pattern of the sample ICS−PMO(F) exhibits a sharp reflection accompanied by two reflections with lower intensities at higher angle ranges, which can be indexed as (100), (110) and (210) diffractions of hexagonal structures, indicating that ICS−PMO(F) is a well-ordered mesoporous material. However, the reflections of (100), (110), and (200) are the three most typical reflections for highly ordered hexagonal mesoporous materials. The lack of the (200) reflection for ICS−PMO(F) may be indicative of some sort of structure transformation. To obtain more information on the structures of ICS−PMO(F), TEM was performed, as illustrated in Figure 2. The hexagonally patterned periodicity of the mesopores was observed if the electron beam was parallel to the pore direction. Moreover, the linelike periodicity of the pores and frameworks was imaged if the electron beam was perpendicular to the pore direction. These results present direct evidence that ICS−PMO(F) exhibits hexagonal mesostructure, similar to that of mesoporous silica SBA-15. In contrast, ICS−PMO(no F) shows only one sharp reflection along with a broad shoulder at a higher angle range, indicating poor mesostructural ordering compared to that of ICS−PMO(F). The above comparison shows that the presence of F^- can significantly improve the quality of the resulting ICS−PMOs. The absence of the (200) reflection for ICS−PMO(F) may be correlated with its highly condensed framework structure.[22] To obtain further evidence, solid-state ^{29}Si MAS NMR was recorded for both samples, as shown in Figure 3. Two strong signals at −59.2 and −67.7 ppm, which can be attributed to the resonances of T^2 [$RSi(OSi)_2OH$] and T^3 [$RSi(OSi)_3$] Si atoms, are well-resolved.[4b,c,23] The intensity of the T^3 signal for ICS−PMO-(F) is apparently more pronounced than that for ICS−

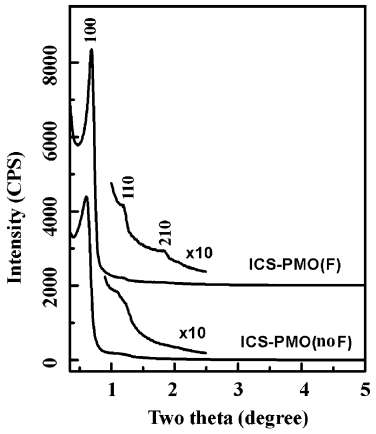

Figure 1. Small-angle XRD patterns of ICS−PMO(F) and ICS−PMO(no F).

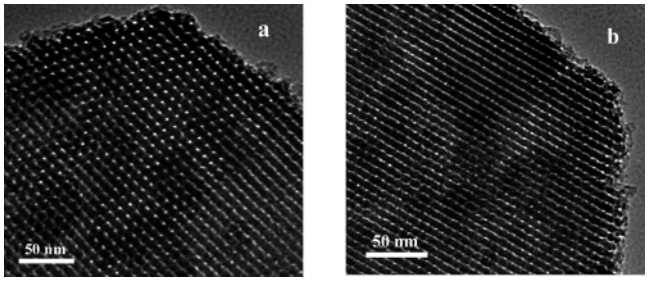

Figure 2. TEM image of ICS−PMO(F). (a) The electron beam is parallel to the pore direction. (b) The electron beam is perpendicular to the pore direction.

(22) (a) Lindén, M.; Blanchard, J.; Schacht, S.; Schunk, S. A.; Schueth, F. *Chem. Mater.* **1999**, *11*, 3002. (b) Impéror-Clerc, M.; Davidson, P.; Davidson, A. *J. Am. Chem. Soc.* **2000**, *122*, 11925. (c) Gross, A. F.; Le, V. H.; Kirsch, B. L.; Riley, A. E.; Tolbert, S. H. *Chem. Mater.* **2001**, *13*, 3571.

(23) Zhou, Z.; Bao, X.; Zhao, X. S. *Chem. Commun.* **2004,**1376.

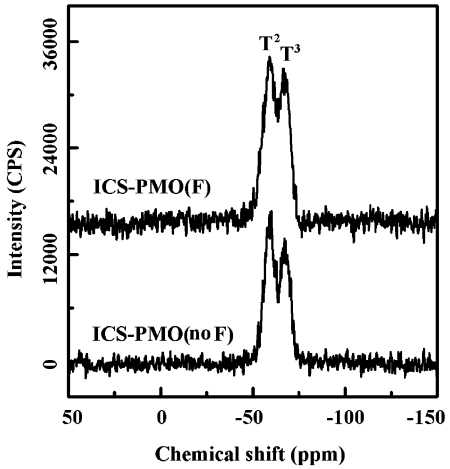

Figure 3. Solid-state ^{29}Si MAS NMR of ICS−PMO(F) and ICS−PMO(no F).

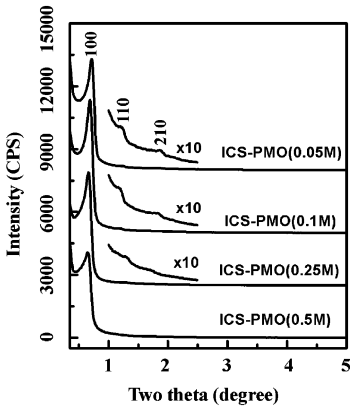

Figure 4. XRD patterns of ICS−PMOs prepared under different acidic solutions.

PMO(no F), confirming that the framework of ICS−PMO(F) is more condensed than that of ICS−PMO(no F).

To optimize synthetic conditions, a series of ICS-bridged PMOs were prepared in HCl solutions with varying concentrations. The XRD patterns of these ICS−PMO materials are shown in Figure 4. It can be observed that decreasing the acidity of the solution resulted in the improvement of both the XRD reflection intensities and the resolution: only one reflection with the lowest intensity was detected for ICS−PMO(0.50 M), indicative of poor mesostructural ordering. In contrast, two XRD reflections are resolved for the ICS−PMO(0.25 M), and three well-resolved reflections for ICS−PMO(0.10 M) and ICS−PMO(0.05 M) have been obtained, indicating well-ordered ICS−PMOs under these less acidic conditions. We have found that white precipitates were immediately produced once ICS−Si was added to the 0.5 M HCl solution. However, it took approximately 15 min to observe the white precipitates if 0.05 M HCl was used as the synthetic medium. Hence, it is expected that the lower hydrolysis rate of ICS−Si in the weaker acidic solution is favorable for the assembly of the P123 surfactant micelles and the organosilicates (resulting from the hydrolysis of ICS−Si). Previous attempts to synthesize PMOs with a large bridged group, such as ICS groups,[13,14] tetraazacyclotetradecane,[16a] Schiff base complexes,[16b,c] and alkoxysilyl-functionalized dendrimers,[12] have afforded materials (either) with a small percentage of the bridged groups (or) and poorly ordered mesostructures. This is due to the fact that the bulky functional groups could significantly reduce the self-assembling ability of the surfactant micelles and organosilicates (resulting from the hydrolysis of the organosilica precursors) by limiting their accommodation into the pore walls, resulting in materials with poor mesostructures or with a low content of the bulky groups. The hydrolysis and condensation of silsesquioxanes is a very complex process. Inductive effects, steric effects, and the polarization properties of the silsesquioxanes impose significant impacts on their hydrolysis and polymerization. A polarized, electron-donating group accelerates the hydrolysis and condensation, while a bulky group always hinders the hydrolysis and polymerization of silsesquioxanes.[24] In the case of ICS−Si, its inductive effect on the Si atom is similar to that of the moiety Si−CH_2CH_2−Si. However, its very large volume apparently hinders its hydrolysis and condensation, which is detrimental to the formation of well-ordered mesostructures. Therefore, the polarization effect may play a critical role in the fast hydrolysis and polymerization of the ICS−Si and subsequent formation of well-ordered ICS−PMO materials. The very fast hydrolysis of ICS−Si is unfavorable for the assembly of the surfactant micelles and organosilicates produced at higher acidic conditions. This is why good ordered products are desirable under reactively weak acidic media for the ICS−PMO in the present experiment. This result is in line with the formation of methylene-bridged PMOs under acidic conditions.[3b] Considering the effect of NH_4F on the quality of the ICS−PMO discussed in the above section, F^- is expected to play a key role in formation of well-ordered ICS−PMO materials. In fact, previous studies have suggested that the existence of small concentrations of F^- is beneficial to the formation of highly ordered siliceous SBA-15.[21,25]

Table 1. Structural Parameters for the ICS−PMOs Prepared under Different Acidic Conditions

	d_{100} (nm)	d_{110} (nm)	d_{200} (nm)	d_{210} (nm)	BET surface area (m^2/g)	pore diam (nm)	pore vol (mL/g)
ICS−PMO(0.05 M)	12.35	7.25		4.68	198.0	5.4	0.25
ICS−PMO(0.10 M)	12.65	7.38		4.86	198.8	5.7	0.27
ICS−PMO(0.25 M)	13.35		6.87		205.7	6.2	0.27
ICS−PMO(0.50 M)	13.34				97.1	7.2	0.14

Figure 5 shows the N_2 adsorption/desorption isotherms and PSDs for the ICS−PMO(*x* M) samples. Structure parameters for these materials are presented in Table 1. All isotherms measured were type IV, with capillary condensation at relative pressures of 0.45−0.78, indicating that these materials exhibit a mesoporous structure.[26] However, the capillary condensation/evaporation steps are significantly less sharp in comparison with those of high-quality SBA-15-like mesoporous materials, suggesting that a certain deterioration of the mesostructures has occurred for these ICS−PMO materials. In addition, all the adsorption isotherms rise slowly at relative pressure above 0.76, implying that textural porosity has been gradually formed.[14,26] Taking into account the N_2

(24) Hook, R. J. *J. Non-Cryst. Solids* **1996**, *195*, 1.
(25) (a) Kim, J. M.; Han, Y.-J.; Chmelka, B. F.; Stucky, G. D. *Chem. Commun.* **2000**, 2437. (b) Schmidt-Winkel, P.; Yang, P.; Margolese, D. L.; Chmelka, B. F.; Stucky, G. D. *Adv. Mater.* **1999**, *11*, 303.
(26) Kruk, M.; Jaroniec, M. *Chem. Mater.* **2001**, *13*, 3169.

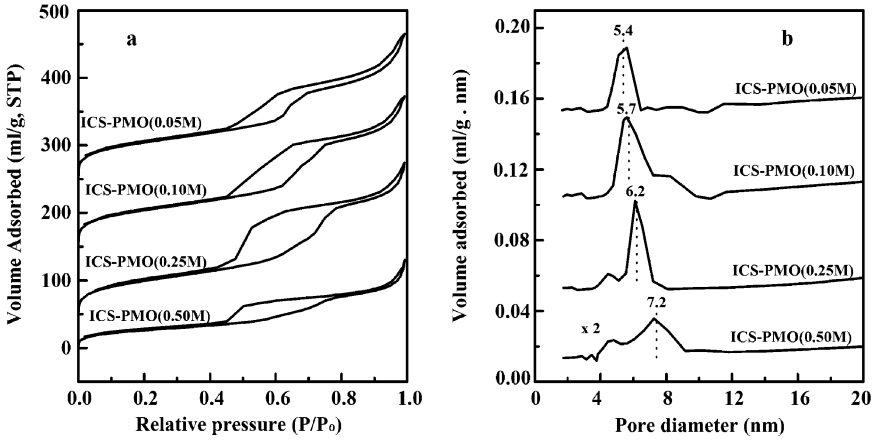

Figure 5. (a) N_2 sortion isotherms and (b) PSDs of the ICS−PMO samples prepared under different acidic conditions.

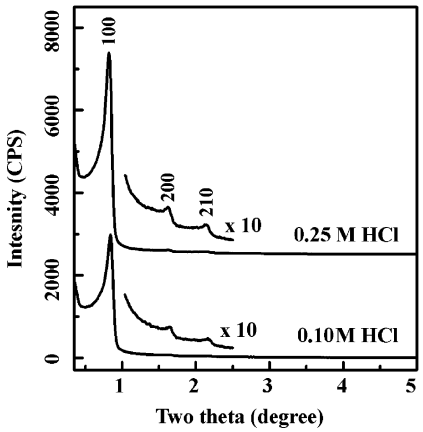

Figure 6. Comparison of small-angle XRD patterns of ICS−Et−PMO-(0.50) synthesized at different acidic conditions. Synthetic parameters: ICS−Si/Et−Si = 0.5/[(3/2)0.5], F/Si = 3.3%.

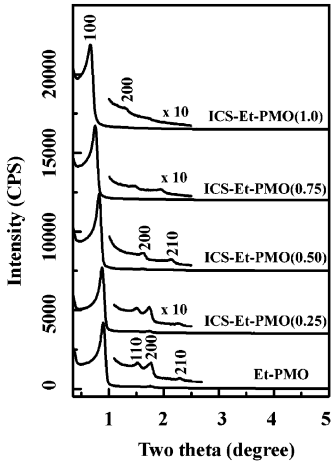

Figure 7. Small-angle XRD patterns for the bifunctionalized ICS−Et−PMOs prepared with different ICS−Si/Et−Si ratios in the synthesis mixtures.

adsorption/desorption properties and the XRD patterns, we conclude that large ICS-group-bridged PMOs with rather well-ordered mesostructures have been prepared. However, their mesostructural ordering is not as perfect as that of high-quality SBA-15. This could be expected due to the fact that the bulky ICS groups are geometrically limited to accommodate the mesopore walls.

(2) Bifunctonalized PMOs Consisting of ICS−Si and Et−Si. To prepare well-ordered bifunctionalized ICS−Et−PMO materials, solution acidity was first optimized under the conditions that the ratio of ICS−Si to Et−Si was kept at 0.5/[(3/2)0.5]. Two samples were prepared in 0.25 and 0.10 M HCl solutions with the aid of NaCl and NH_4F. XRD patterns illustrated in Figure 6 show that the bifunctionalized ICS−Et−PMO prepared in 0.25 M HCl solution exhibits significantly higher intensities than the corresponding sample prepared in 0.10 M HCl solution. It took approximately 2 min for ICS−Si to hydrolyze in 0.10 M HCl solution to produce a white precipitate. In contrast, it took almost 24 min for precipitation to occur in the case of Et−Si. However, ICS−Si produced a white precipitate within 1 min and Et−Si within 7 min in a 0.25 M HCl solution. The decreased difference in the hydrolysis rates for ICS−Si and Et−Si under higher acidic conditions is likely to be responsible for the significantly better mesostructural ordering of the obtained products. Therefore, the 0.25 M HCl solution was used for further study.

Figure 7 presents the XRD patterns of the bifunctionalized ICS−Et−PMO prepared with different contents of ICS−Si and Et−Si in the synthetic precursors. It is obvious that the higher contents of ICS−Si resulted in larger cell dimensions of the mesostructured products, indicative of the simultaneous incorporation of ICS−Si and Et−Si in each preparation. This is due to the fact that the volume of ICS−Si is much larger than that of Et−Si. Et−PMO [namely, ICS−Et−PMO(0.0)] and ICS−Et−PMO(0.25) show four reflections, indexed as (100), (110), (200), and (210), confirming that Et−PMO and ICS−Et−PMO(0.25) are highly ordered mesoporous materials with typically two-dimensional hexagonal mesostructures (*P*6*mm*).[27] Increasing the concentrations of ICS−Si in the precursors reduces the structural ordering of the products. Only three reflections can be resolved for ICS−Et−PMO-(0.50) and ICS−Et−PMO(0.75). These reflections could be assigned either to (100), (200), and (210) of the hexagonal structure (*P*6*mm*) or to (110), (200), and (321) of the cubic structure ($I4_132$). The lack of the (110) diffraction characteristic of *P*6*mm* has been suggested to be evidence that the structure is cubic.[14] To ascertain the structure, TEM was performed on the sample ICS−Et−PMO(0.50), as shown in Figure 8. The image in Figure 8a, which was taken with the

(27) Zhao, D. Y.; Feng, J. L.; Huo, Q. S.; Melosh, N.; Fredrickson, G. H.; Chmelka, B. F.; Stucky, G. D. *Science* **1998**, *279*, 548.

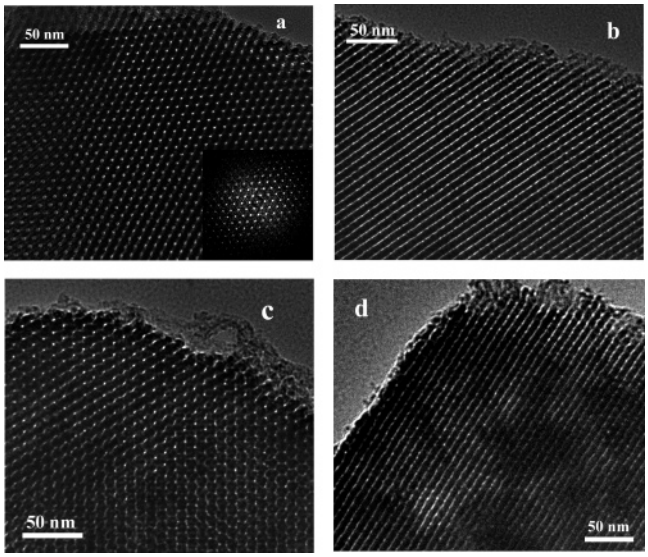

Figure 8. TEM images of (a, b) the bifunctionalized ICS−Et−PMO(0.50) and (c, d) ICS−Et−PMO(1.0). (a, c) The electron beam is parallel to the pore direction. The inset in (a) is the corresponding diffraction patterns made by Fourier transform. (b, d) The electron beam is perpendicular to the pore direction.

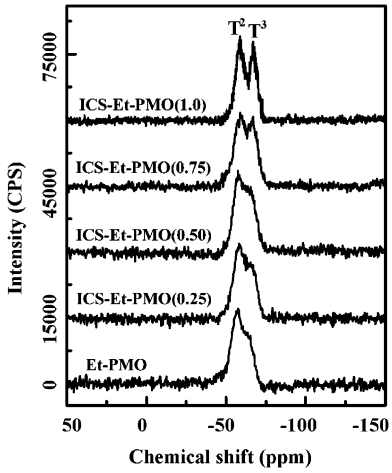

Figure 9. Solid-state ^{29}Si MAS NMR spectra for the bifunctionalized ICS−Et−PMO prepared with different ICS−Si/Et−Si ratios in the synthesis mixtures.

electron beam parallel to the pore direction, **s**hows highly ordered, hexagonal arrays of mesopores, and the image in Figure 8b, which was taken with the electron beam perpendicular to the pore direction, presents the linelike image of the pores. Fourier transform diffractions for image a (inset in Figure 8a) provides direct evidence that the pore arrays of ICS−Et−PMO(0.50) are hexagonally symmetrical. These results clearly demonstrate that, despite the absence of the (110) reflection in the XRD patterns, ICS−Et−PMO(0.50) exhibits two-dimensional hexagonal mesostructures. Similar results were also obtained for ICS−Et−PMO(1.0) (in Figure 8c,d).

^{29}Si MAS NMR spectra for ICS−Et−PMO are shown in Figure 9. The resonances of T^2 [$RSi(OSi)_2OH$] and T^3 [$RSi(OSi)_3$] Si atoms were well-resolved. Decreasing the content of ICS−Si in the synthetic precursors resulted in the steady reduction of the T^3 signals, indicating that the framework condensation of the ICS−Et−PMOs was reduced upon decreasing the ICS−Si contents. The lack of Q^n signals

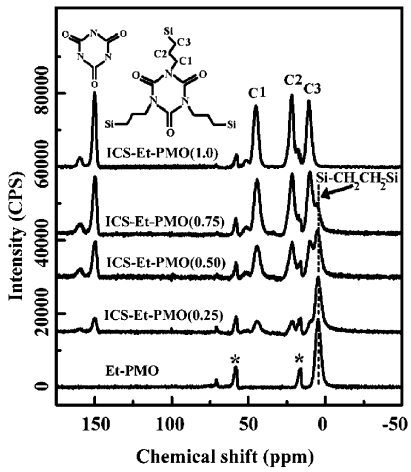

Figure 10. Solid-state ^{13}C MAS NMR spectra for the bifunctionalized ICS−Et−PMO prepared with different ICS−Si/Et−Si ratios in the synthesis mixtures. An asterisk indicates a peak arising from the carbon in the surface ethoxy groups $-OCH_2CH_3$.

[$Si(OSi)_n(OH)_{4-n}$, $n = 2-4$] between −90 and −120 ppm confirms that all Si atoms are connected to C atoms, and no Si−C bond cleavage occurred during the synthesis and solvent extraction. ^{13}C MAS NMR spectra for the ICS−Et−PMOs are depicted in Figure 10. The signal at 150.7 ppm is assigned to the carbons in the isocyanurate rings (inset of Figure 10).[28] The bands at 11.1, 22.0, and 45.8 ppm are attributed to C3, C2, and C1 in the propyl groups bridged to the isocyanurate rings and Si atoms in the ICS−Si (inset in Figure 10).[29] The resonance at 5.1 ppm arises from carbons in Et−Si.[4] Both the signals of ICS−Si and Et−Si are clearly observed for the three bifunctionalized samples ICS−Et−PMO(0.75), ICS−Et−PMO(0.50), and ICS−Et−PMO(0.25). The signal intensities of ICS−Si are steadily reduced with a steady decrease its contents, which is accompanied by the steady enhancement of the signal intensity of Et−Si. These results strongly suggest that the bifunctionalized ICS−Et−PMOs have indeed been obtained using the mixture of ICS−Si and Et−Si, with a very wide component variation, as coprecursors. Additionally, the two weak signals at 17.5 and 58.6 ppm are assigned to the carbons in the surface ethoxy groups ($Si-OCH_2CH_3$, marked by asterisks in Figure 10), which were formed during surfactant extraction by acidified ethanol.[3b,4a,c] Also, these signals could originate from physisorbed/chemisorbed ethanol as well, especially if the samples were not dried well. The intensities of both signals tend to be enhanced with rising content of Et−Si, which may be attributable to the fact that a higher content of Et−Si in the precursors resulted in materials with less condensed pore walls, namely, a higher density of T^2 Si atoms that can be anchored by the $-OCH_2CH_3$ groups (see ^{29}Si MAS NMR in Figure 9). Considering the big difference in volumes of the ICS− group and Et− groups, and the big difference in the hydrolysis rates between ICS−Si and Et−Si, it is expected that a number of bifunctionalized PMOs, consisting of different bridged organosilanes, could be prepared by

(28) Damodaran, K.; Sanjayan, G. J.; Rajamohanan, P. R.; Ganapathy, S.; Ganesh, K. N. *Org. Lett.* **2001**, *3*, 1921.
(29) (a) Cestaric, A. R.; Airoldi, C. *Langmuir* **1997**, *13*, 2681. (b) Huh, S.; Wiench, J. W.; Yoo, J.-C.; Pruski, M.; Lin, V. S.-Y. *Chem. Mater.* **2003**, *15*, 4247.

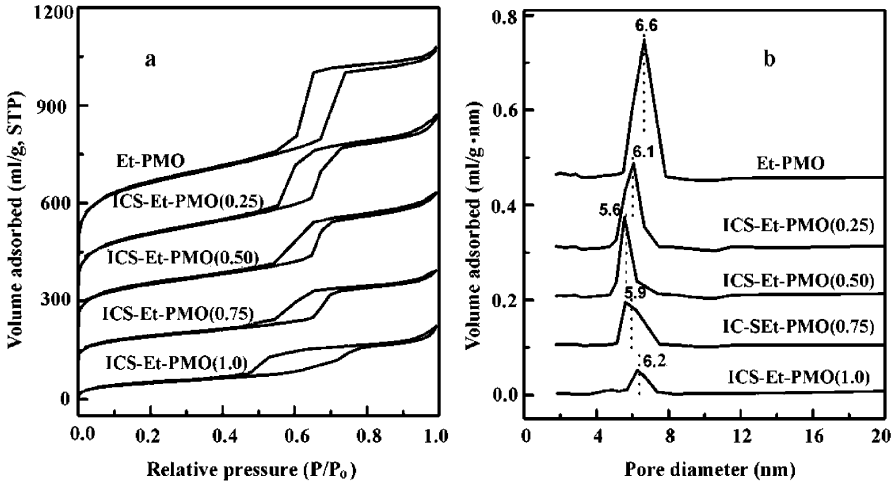

Figure 11. N_2 sorption isotherms (a) and pore size distributions (b) for the bifunctionalized ICS−Et−PMO prepared with different ICS−Si/Et−Si ratios in the synthesis mixtures.

Table 2. Structural Parameters for the ICS−Et−PMOs Prepared with Different Contents of ICS−Si/Et−Si in the Precursors

	d_{100} (nm)	d_{110} (nm)	d_{200} (nm)	d_{210} (nm)	BET surface area (m^2/g)	pore diam (nm)	pore vol (mL/g)
ICS−Et−PMO(1.0)	13.35		6.87		205.7	6.2	0.27
ICS−Et−PMO(0.75)	11.8		6.00	4.53	331.3	5.9	0.35
ICS−Et−PMO(0.50)	10.76		5.45	4.12	544.2	5.6	0.49
ICS−Et−PMO(0.25)	10.17	5.87	5.09	3.87	738.4	6.1	0.63
Et−PMO	10.07	5.85	5.05	3.86	940.6	6.6	0.72

Table 3. Elemental Analysis of the ICS−Et−PMOs

	N content (wt %)		C content (wt %)		$n_{(ICS-Si)}/n_{(Et-Si)}$[a]	
	measd	calcd	measd	calcd	measd	calcd
ICS−Et−PMO(1.0)	9.93	10.29	34.86	35.29	1.0/0.0	1.0/0.0
ICS−Et−PMO(0.75)	8.60	9.29	32.97	33.63	1.4/1.0	2.0/1.0
ICS−Et−PMO(0.50)	6.42	7.78	29.95	31.11	0.46/1.0	0.67/1.0
ICS−Et−PMO(0.25)	3.36	5.22	25.61	26.87	0.14/1.0	0.22/1.0
Et−PMO			20.29	18.18	0.0/1.0	0.0/1.0

[a] $n_{ICS-Si}/n_{Et-Si} = (1 - x)/[(3/2)x]$ ($x = 0.25, 0.50, 0.75$) for the three biofunctionalized samples.

drawing the hydrolysis rates of the organosilica precursors to match each other in a surfactant environment.

Figure 11 displays N_2 sorption isotherms and PSDs for the ICS−Et−PMOs. The corresponding structural parameters are presented in Table 2. All the isotherms for the Et−Si-containing samples are type IV in classification,[26] displaying sharp capillary condensation at relative pressures of 0.45−0.75. The hysteresis loop, with parallel and nearly vertical branches in all of the isotherms except for ICS−Et−PMO-(1.0), is type H1 hysteresis, characteristic of materials with a high degree of pore size uniformity. The capillary condensation/evaporation steps became sharper with increasing content of Et−Si, reflecting an improvement of the mesopore ordering.[26] The BET surface areas and mesopore volumes steadily increase with increasing content of Et−Si, demonstrating again that both ICS−Si and Et−Si were proportionately accommodated into the frameworks of the materials in this study. Therefore, bifunctionalized ICS−Et−PMOs have been successfully prepared with a wide range of component variation of ICS−Si and Et−Si.

Elemental analysis of the ICS−Et−PMOs further confirms the presence of ICS−Si and Et−Si in them. It seems that not all of the ICS−Si in the mixed precursors (of ICS−Si and Et−Si) has indeed been incorporated into the frameworks of ICS−Et−PMOs (see Table 3). One reason for the lower nitrogen contents is that the $-OCH_2CH_3$ groups, formed on the pore surfaces of PMOs during the surfactant extraction, contribute to higher carbon contents than the theoretic values estimated from the precursor compositions, resulting in the lower estimation of the incorporation of ICS−Si in the bifunctionalized product.

(3) Application of ICS−PMOs for Embedding Metal Nanoparticles. We have recently demonstrated that PMOs as host materials are advantageous over mesoporous silica in formation of highly crystalline Ge nanocrystals.[3b] The ICS-containing mesoporous silica has been demonstrated to exhibit a high capacity to adsorb Hg^{2+}.[13a] Because of the importance of Pt nanocrystals in the nanochemistry of OMMs and their application in catalysis,[30] we have tested the possibility of using ICS−PMO(0.10 M) as a host, *without surface modification by other specific functional groups*,[19] to adsorb H_2PtCl_6 and then to prepare Pt nanocrystals within

(30) (a) Song, H.; Rioux, R. M.; Hoefelmeyer, J. D.; Komor, R.; Niesz, K.; Grass, M.; Yang, P.; Somorjai, G. A. *J. Am. Chem. Soc.* **2006**, *128*, 3027. (b) Yang, C.-M.; Liu, P.-H.; Ho, Y.-F.; Chiu, C.-Y.; Chao, K.-J. *Chem. Mater.* **2003**, *15*, 275. (c) Zhang, L.-X.; Shi, J.-L.; Yu, J.; Hua, Z.-L.; Zhao. X.-G.; Ruan. M.-L. *Adv. Mater.* **2002**, *14*, 1510. (d) Yang, C. M.; Sheu, H. S.; Chao, K. J. *Adv. Funct. Mater.* **2002**, *12*, 143. (e) Rioux, R. M.; Song, H.; Hoefelmeyer, J. D.; Yang, P.; Somorjai, G. A. *J. Phys. Chem. B* **2005**, *109*, 2192. (f) Wakayama, H.; Setoyama, N.; Fukushima, Y. *Adv. Mater.* **2003**, *15*, 742.

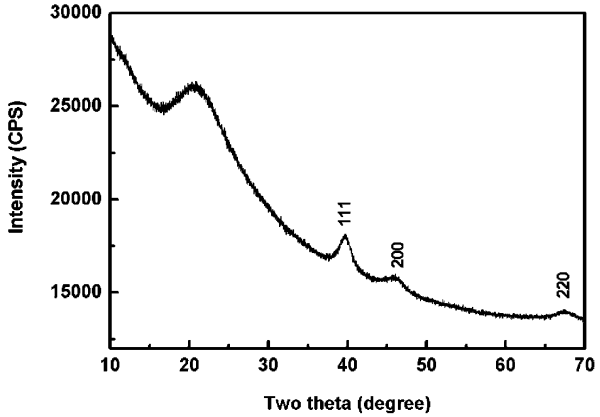

Figure 12. Wide-angle XRD pattern of the sample Pt−ICS−PMO.

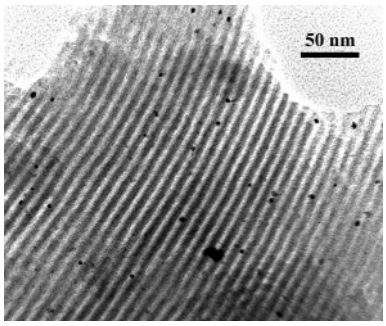

Figure 13. TEM image of the sample Pt−ICS−PMO.

their mesopores by $NaBH_4$ reduction as described in the Experimental Section.

The Pt-containing sample Pt−ICS−PMO reveals a very similar small-angle XRD pattern as compared with the host ICS−PMO(0.10 M). The wide-angle XRD pattern of Pt−ICS−PMO is presented in Figure 12. The three reflections centered at 39.7°, 46.1°, and 67.4° can be attributed to (111), (200), and (200) diffractions of the facet-centered cubic lattice of metallic Pt. The broadening of XRD reflections indicates that the Pt particles fabricated inside ICS−PMO are nanodimensional, and the average size is estimated to be less than 5 nm, consistent with the pore size of 5.7 nm for ICS−PMO(0.10 M). To gain insight into the existence of Pt within the ICS−PMO host, Figure 13 shows a TEM image of Pt−ICS−PMO. A number of Pt nanoparticles were directly imaged as black dots within the channels and within the frameworks. Only a few large particles were also observed on the external surfaces of the ICS−PMO host. Energy dispersive spectroscopy (EDS) analysis showed an atom ratio of Si to Pt of 52.01/1.23. Considering the fact that three Si atoms correspond to one ICS group, the molar ratio of ICS to Pt groups is ∼14/1, indicating that only a small portion of the ICS groups have adsorbed H_2PtCl_6. This may be because of the fact that most of the ICS groups in the present experiment are located inside the pore walls, and it is not easy for these ICS groups to be accessible to the H_2PtCl_6 in the solution. In addition, the negative charging of the $PtCl_6^{2-}$ anion may also be disadvantageous for the adsorption process compared with that of typical aqua complexes of metal cations, which are positively charged. Preliminary tests of the adsorption of Zn^{2+} by the ICS−PMO gave a molar ratio of ICS to Zn^{2+} of approximately 9/1. Expectedly the content of Zn is indeed higher than that of Pt. A more detailed comparison of the adsorption properties of our ICS−PMO materials with similar systems is under way.

Conclusion

An efficient approach to synthesize ICS−PMOs and bifunctionalized PMOs consisting of two types of bridged organosilane groups, ICS−Et−PMOs, has been exploited using surfactant P123 as a template under acidic conditions in the presence of inorganic additives. It is suggested that F^- ions play an important role in the synthesis of bifunctionalized ICS−Et−PMOs: they can significantly accelerate the hydrolysis rate of Et−Si to match that of ICS−Si, resulting in highly ordered PMOs with two types of bridged groups. H_2PtCl_6 was adsorbed by the ICS−PMOs, and Pt nanocrystals were subsequently prepared within the pores of the ICS−PMO materials. We have presented a simple but efficient scheme to prepare bifunctionalized PMOs with different bridged groups. We believe the present strategy could be extended into preparing a large number of PMOs with multifunctional bridged groups.

Acknowledgment. W.-H.Z. thanks the Alexander von Humboldt Foundation for a fellowship. F.S. is grateful for a stipend from the German National Academic Foundation. The work was further supported by the German Research Foundation (DFG) within the framework of the Research Centre on Metal Support Interaction in Heterogeneous Catalysis (Grant SFB-558) at the Ruhr-University Bochum.

CM061922P